

Two isozymes of particulate methane monooxygenase with different methane oxidation kinetics are found in *Methylocystis* sp. strain SC2

Mohamed Baani and Werner Liesack*

Department of Biogeochemistry, Max Planck Institute for Terrestrial Microbiology, Karl-von-Frisch-Strasse, 35043 Marburg, Germany

Edited by David M. Karl, University of Hawaii, Honolulu, HI, and approved May 21, 2008 (received for review March 23, 2007)

Methane-oxidizing bacteria (methanotrophs) attenuate methane emission from major sources, such as wetlands, rice paddies, and landfills, and constitute the only biological sink for atmospheric methane in upland soils. Their key enzyme is particulate methane monooxygenase (pMMO), which converts methane to methanol. It has long been believed that methane at the trace atmospheric mixing ratio of 1.75 parts per million by volume (ppmv) is not oxidized by the methanotrophs cultured to date, but rather only by some uncultured methanotrophs, and that type I and type II methanotrophs contain a single type of pMMO. Here, we show that the type II methanotroph *Methylocystis* sp. strain SC2 possesses two pMMO isozymes with different methane oxidation kinetics. The *pmoCAB1* genes encoding the known type of pMMO (pMMO1) are expressed and pMMO1 oxidizes methane only at mixing ratios >600 ppmv. The *pmoCAB2* genes encoding pMMO2, in contrast, are constitutively expressed, and pMMO2 oxidizes methane at lower mixing ratios, even at the trace level of atmospheric methane. Wild-type strain SC2 and mutants expressing *pmoCAB2* but defective in *pmoCAB1* consumed atmospheric methane for >3 months. Growth occurred at 10–100 ppmv methane. Most type II but no type I methanotrophs possess the *pmoCAB2* genes. The apparent K_m of pMMO2 (0.11 μM) in strain SC2 corresponds well with the $K_{m(\text{app})}$ values for methane oxidation measured in soils that consume atmospheric methane, thereby explaining why these soils are dominated by type II methanotrophs, and some by *Methylocystis* spp., in particular. These findings change our concept of methanotroph ecology.

atmospheric methane | methanotrophs | *pmoA*

Methane (CH_4) is present in the atmosphere at a mixing ratio of ≈ 1.75 parts per million by volume (ppmv) (1). It is 20–23 times more effective as a greenhouse gas than carbon dioxide, and its atmospheric concentration over the past two centuries has increased at a rate of $\approx 1\%$ per year (2). Methane-oxidizing bacteria, or methanotrophs, are crucial players in the global cycle of the greenhouse gas methane. They are strict aerobes that use methane as their only source of carbon and energy. The bacteria oxidize methane to formaldehyde, which is then either assimilated into cell biomass or further oxidized to carbon dioxide.

Cultured methanotrophs are classified into types I and II, which differ in the intracellular membrane arrangement, pathways of carbon assimilation, and phospholipid fatty acid (PLFA) composition (3). Type II methanotrophs of the genera *Methylocystis* and *Methylosinus* form a distinct clade within the *Alphaproteobacteria*, whereas the 10 genera currently recognized as type I methanotrophs belong to the *Gammaproteobacteria*. These well known type I and type II methanotrophs typically inhabit the aerobic interfaces of methanogenic environments, such as natural wetlands and rice paddies, and reduce the potential methane flux to the atmosphere (3–5). Because of the usually high methane supply in these environments, methane is oxidized with low apparent half-saturation constants ($K_{m(\text{app})} > 1 \mu\text{M CH}_4$). These K_m values are similar to those determined for cultured methanotrophs ($K_{m(\text{app})} = 2\text{--}12 \mu\text{M CH}_4$) (6, 7).

In upland soils, methanotrophic bacteria take up methane directly from the atmosphere (3, 6, 8, 9). Methane consumption in these soils is a small but a significant part of the global methane budget, comparable in magnitude to the estimated excess of emissions over sinks in recent years (29 Tg year⁻¹) (9). In contrast to methanotrophs in the aerobic interfaces of methanogenic environments, the methanotrophs active in dry, well aerated upland soils, for example, forest soils, consume methane with high apparent affinity ($K_{m(\text{app})}$ values of 0.01–0.28 $\mu\text{M CH}_4$) (6). Molecular studies have indicated the presence of type II methanotrophs in most upland soils (10, 11) and have provided increasing evidence that, in these soils, the most abundant methanotrophs belong to several uncultivated groups, including upland soil cluster α (USC α) and upland soil cluster γ (USC γ) (10, 12, 13). Members of USC α and USC γ are presumed to be specialized oligotrophs adapted to living solely on atmospheric methane. The methanotrophs cultured to date, however, were thought to be incapable of surviving and remaining active at the trace level of atmospheric methane because of their low affinity for methane.

In the methane-oxidation pathway in all known methanotrophs, except *Methylocella* spp., the first step is mediated by particulate methane monooxygenase (pMMO) (14, 15). pMMO catalyzes the conversion of methane to methanol. This copper-dependent enzyme is synthesized even when only a minuscule amount of copper is available (16, 17). Under copper-limiting conditions, a subset of the methanotrophs produce a soluble type of MMO (sMMO) (4, 16), an enzyme evolutionarily distinct from pMMO (15). However, to initiate synthesis of pMMO under copper-limiting conditions, some methanotrophs may be able to mobilize and acquire copper from mineral and organic solid phases by releasing the fluorescent chromopeptide methanobactin (17, 18).

The operon encoding pMMO consists of three consecutive ORFs (*pmoC1*, *pmoA1*, and *pmoB1*; *pmoCAB1*). Two nearly sequence-identical copies of *pmoCAB1* are found in both type I and type II methanotrophs (15, 19). Each of the *pmoCAB1* operons is transcribed to form a polycistronic mRNA of 3.3 kb (16), which is translated to form the $\alpha_3\beta_3\gamma_3$ main component of functionally active pMMO, particulate methane hydroxylase (pMH) (20). Because pMMO is an integral part of the intracytoplasmic membranes, its crystal structure remained elusive for many years (20). The exact catalytic mechanism of methane oxidation is still hypothetical, involving both activation of oxygen and oxidation of methane (20, 21).

An unusual type of pMMO has recently been detected in the filamentous methanotroph *Crenothrix polyspora*. This gammapro-

Author contributions: W.L. designed research; M.B. performed research; and W.L. wrote the paper.

The authors declare no conflict of interest.

This article is a PNAS Direct Submission.

*To whom correspondence should be addressed. E-mail: liesack@mpi-marburg.mpg.de.

This article contains supporting information online at www.pnas.org/cgi/content/full/0702643105/DCSupplemental.

© 2008 by The National Academy of Sciences of the USA

Table 1. pMMO mutants generated from wild-type *Methylocystis* sp. strain SC2 and used in this study

Mutant	Relevant trait(s)
SC2-P1	$\Delta pmoCAB1::kan$ mutant, deleted in one of the two copies of <i>pmoCAB1</i>
SC2-P2	$\Delta pmoCAB1a::kan, \Delta pmoCAB1b::kan$ mutant, deleted in both copies of <i>pmoCAB1</i> (lacking pMMO1)
SC2-P3	$\Delta pmoCAB2::kan$ mutant, deleted in <i>pmoCAB2</i> (lacking pMMO2)
SC2-P4*	$\Delta pmoCAB1a::kan, \Delta pmoCAB1b::kan, \Delta pmoCAB2::tet$ mutant, deleted in both copies of <i>pmoCAB1</i> and in <i>pmoCAB2</i> (lacking both pMMO1 and pMMO2)

**pmo* null mutant: growth on methanol but not on methane.

teobacterium is closely related to type I methanotrophs. Comparative analysis of *pmoA* gene sequences, however, showed that its deduced PmoA sequence forms a lineage distinct from the monophyletic branch of type I methanotrophs (22).

The current concept of methanotrophy presumes that culturable type I and type II methanotrophs harbor a single type of pMMO. However, in *Methylocystis* sp. strain SC2, we recently identified, in addition to two copies of *pmoCAB1*, a *pmoCAB*-like gene cluster (*pmoC2*, *pmoA2*, *pmoB2*; *pmoCAB2*) with only a low degree of identity to *pmoCAB1* at both the nucleotide (67.4–70.9%) and derived amino acid (59.3–65.6%) sequence levels (23). We have shown by using a PCR-based survey that *pmoCAB2* is widely but not universally distributed among type II methanotrophs, and is not present in representative type I methanotrophs of the genera *Methylobacter*, *Methylomicrobium*, *Methylomonas*, *Methylococcus*, and *Methylocaldum* (24). The latter two genera are also referred to as type X methanotrophs, a subset of type I methanotrophs that is distinguished by certain physiological, biochemical, and phylogenetic characteristics (3, 25). Among a collection of 27 type II methanotroph strains, 19 strains have *pmoCAB2*, including most *Methylocystis* spp. (12 of 16), all strains of *Methylosinus sporium* (4 of 4), and some strains of *Methylosinus trichosporium* (3 of 7). *pmoA2* sequences obtained from these cultured type II methanotrophs form a coherent phylogenetic cluster distinct from that of *pmoA1* (24). The calculation of the relative rate of nonsynonymous (amino acid-changing) to synonymous (non-amino acid-changing) nucleotide substitutions of *pmoA1* and *pmoA2* sequences indicates that, in recent evolutionary history, a strong purifying selection has been acting on both genes (24). These results provided strong evidence that the gene product of *pmoA2* plays an important

functional role in type II methanotrophs, but the exact nature of its function remained unknown. We used *Methylocystis* sp. strain SC2 as a model organism to elucidate this function. Here, we demonstrate that *pmoCAB1* and *pmoCAB2* encode two pMMO isozymes with different methane oxidation kinetics.

Results and Discussion

Construction of Mutant Strains Defective in *pmoCAB* Expression.

Sequence-specific fusion PCR enabled the construction of mutant strains defective in a single copy (SC2-P1) or both copies (SC2-P2) of *pmoCAB1*, in *pmoCAB2* (SC2-P3), and in both copies of *pmoCAB1* and in *pmoCAB2* (SC2-P4) (Table 1). A kanamycin- or tetracycline-resistance marker cassette replaced the target gene(s). The gene deletions and marker insertions were confirmed by diagnostic PCR (data not shown) and Southern hybridization [supporting information (SI) Fig. S1].

Mutant SC2-P4, defective in both copies of *pmoCAB1* and in *pmoCAB2*, grew on methanol but not on methane. Because *Methylocystis* sp. strain SC2 does not produce sMMO (4), this inability of mutant SC2-P4 to use methane provided proof that no other, unknown *pmo* operon was located on its genome.

Growth Experiments under High Methane Mixing Ratios. The growth of wild-type and mutants with 10–15% methane in the headspace was compared to determine whether the conventional pMMO1 protein and the novel pMMO2 protein were active (Fig. 1A). Wild-type strain SC2 and the *pmoCAB2* mutant SC2-P3 grew exponentially after a lag phase of ≈ 4 days. Mutant SC2-P1, defective in only one copy of *pmoCAB1*, grew at a lower rate than wild-type strain SC2 and mutant SC2-P3, which indicates that the

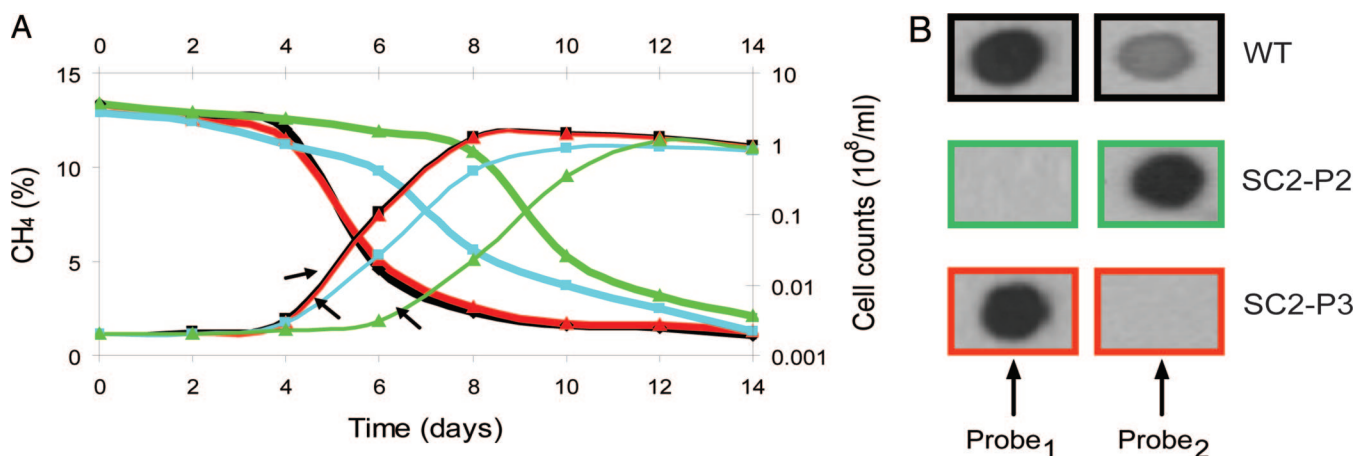


Fig. 1. Methane consumption and growth curves of wild-type *Methylocystis* sp. strain SC2 and its mutants SC2-P1, SC2-P2, and SC2-P3, shown in relation to the expression of *pmoCAB1* and *pmoCAB2* mRNA transcripts during exponential growth on methane. (A) Methane consumption (% vol/vol) over time (solid lines) and cell numbers calculated from OD₆₀₀ measurements: wild-type (black); mutant SC2-P1, defective in a single copy of *pmoCAB1* (blue); mutant SC2-P2, defective in both copies of *pmoCAB1* (green); and mutant SC2-P3, defective in *pmoCAB2* (red). The *pmoCAB* null mutant SC2-P4 and uninoculated controls were used as negative growth controls; the methane concentration did not decline in these controls. (B) *pmoCAB1* and *pmoCAB2* expression detected by Northern blot hybridization of total RNA of wild-type strain SC2 (WT) and mutant strains SC2-P2 and SC2-P3. Total RNA was extracted from aliquots of cultures of wild-type strain SC2 and mutant strains in the early exponential growth phase (arrows, Fig. 1A). Gene probes specifically targeted transcripts of either *pmoCAB1* (Probe₁) or *pmoCAB2* (Probe₂). For target specificity of Probe₁ and Probe₂, see Fig. S1.

Table 2. Methane consumption and growth rates of *Methylocystis* sp. strain SC2 and mutant strains SC2-P1, SC2-P2, and SC2-P3 during incubation at high methane concentrations

Strain	Growth rate, h ⁻¹	Doubling time, h	CH ₄ oxidation rate, 10 ⁻⁸ μmol·cell ⁻¹ ·h ⁻¹
Wild-type	0.074 ± 0.001*	9.4 ± 0.11*	400.6 ± 29.61*
	0.073 ± 0.006 [†]	9.6 ± 0.82 [†]	457.9 ± 136.12 [†]
	0.068 ± 0.001 [‡]	10.1 ± 0.23 [‡]	352.3 ± 29.23 [‡]
SC2-P1	0.045 ± 0.002*	15.4 ± 0.5*	403.9 ± 27.7*
	0.046 ± 0.003 [†]	15.2 ± 1.0 [†]	387.6 ± 63.5 [†]
	0.049 ± 0.002 [‡]	14.2 ± 0.6 [‡]	468.3 ± 81.6 [‡]
SC2-P2	0.041 ± 0.001*	16.8 ± 0.2*	381.6 ± 59.6*
	0.041 ± 0.002 [†]	17.0 ± 0.9 [†]	360.3 ± 50.2 [†]
	0.042 ± 0.003 [‡]	16.6 ± 1.1 [‡]	382.4 ± 60.6 [‡]
SC2-P3	0.071 ± 0.002*	9.7 ± 0.2*	428.8 ± 11.01*
	0.072 ± 0.002 [†]	9.7 ± 0.3 [†]	441.8 ± 3.52 [†]
	0.069 ± 0.002 [‡]	10.1 ± 0.3 [‡]	414.5 ± 16.93 [‡]

Parameters were measured during the early exponential growth phase, which occurred between days 4 and 6 after inoculation for wild-type strain SC2 and mutants SC2-P1 and SC2-P3 and between days 6 and 8 after inoculation for mutant SC2-P2 (Fig. 1).

††Growth rate, doubling time[†], and methane oxidation rate[‡] per cell shown for three independent growth experiments under a headspace of 10–15% (vol/vol) CH₄. Data given for each replicate experiment are means of triplicates ± one standard error of mean.

expression of both copies of *pmoCAB1* is essential for maximum growth. Mutant SC2-P2, defective in both copies of *pmoCAB1*, grew after a lag phase of ≈6 days and concomitantly oxidized methane; therefore, *pmoCAB2* encodes an active pMMO.

We determined the expression of *pmoCAB1* and *pmoCAB2* in cultures of wild-type strain SC2 and mutants SC2-P2 and SC2-P3 in the early exponential growth phase by Northern blot hybridization of total RNA. Both *pmoCAB1* and *pmoCAB2* were expressed in wild-type strain SC2 during growth with 10–15% methane in the headspace, and *pmoCAB1* was expressed at a higher level than *pmoCAB2* (Fig. 1B). As expected, mutant SC2-P2 expressed only *pmoCAB2*, and mutant SC2-P3 expressed only *pmoCAB1*. However, the transcript level of *pmoCAB2* was much higher in mutant SC2-P2 than in the wild-type; the transcript level of *pmoCAB1* in wild-type and mutant SC2-P3 cells appeared to be similar.

The growth rates of mutants SC2-P1 and SC2-P2 during the early exponential phase and correspondingly their doubling times were significantly lower than those of wild-type strain SC2 and mutant SC2-P3 (Table 2). This finding substantiates the conclusion above that, for maximum growth, both copies of *pmoCAB1* must be expressed. The methane oxidation rates per cell of mutants SC2-P1 and SC2-P2, in contrast, were similar to those of wild-type strain SC2 and mutant SC2-P3. Apparently, mutant SC2-P2 is in a nonnative, unbalanced metabolic state owing to the deletion of both copies of *pmoCAB1*. This may have changed the physiological architecture and resulted in an artificial cell response to compensate for the complete deletion of pMMO1 by increased synthesis of pMMO2. However, the increase in *pmoCAB2* transcription (Fig. 1B) and subsequently in methane oxidation activity did not provide mutant SC2-P2 with the same growth rate as wild-type strain SC2 or mutant SC2-P3.

Growth Experiments under Low Methane Mixing Ratios. The differences in the growth responses of mutants SC2-P2 and SC2-P3 under high methane mixing ratios led us to assume that (i) pMMO1 and pMMO2 have different functional roles and (ii) the primary role of pMMO1 is to be active at high methane concentrations. Our assumptions were confirmed by growth experiments carried out at successively lower methane concentrations (Table 3) to determine the threshold levels of methane required for growth and survival of

Table 3. Growth of wild-type *Methylocystis* sp. strain SC2 and mutants at various low mixing ratios of methane (1,000–1.75 ppmv), based on changes in pseudo-first-order rate constants [10^{-6} liter·(ml culture)⁻¹·h⁻¹] of methane oxidation over time

Strain*	Initial rate constant [†]	Final rate constant [‡]	Incubation period, weeks	Growth [§]
1,000 ppmv				
Wild-type	512 ± 21	4,953 ± 213	3	+
SC2-P1	414 ± 16	2,512 ± 34	3	+
SC2-P2	212 ± 26	1,392 ± 24	3	+
SC2-P3	497 ± 31	4,894 ± 10	3	+
700 ppmv				
Wild-type	451 ± 13	4,248 ± 17	3	+
SC2-P1	236 ± 11	2,135 ± 19	3	+
SC2-P2	195 ± 24	1,358 ± 26	3	+
SC2-P3	423 ± 20	4,193 ± 18	3	+
600 ppmv				
Wild-type	384 ± 19	2,053 ± 32	3	+
SC2-P1	351 ± 16	1,594 ± 25	3	+
SC2-P2	289 ± 24	1,289 ± 27	3	+
SC2-P3	296 ± 38	<1	3	-
100 ppmv				
Wild-type	351 ± 56	1,549 ± 24	5	+
SC2-P1	339 ± 37	1,640 ± 100	5	+
SC2-P2	210 ± 23	1,295 ± 19	5	+
SC2-P3	342 ± 37	<1	5	-
10 ppmv				
Wild-type	102 ± 7	74 ± 3	5	±
SC2-P1	97 ± 5	82 ± 12	5	±
SC2-P2	112 ± 21	80 ± 14	5	±
SC2-P3	99 ± 11	<1	5	-
1.75 ppmv				
Wild-type	82 ± 12	11 ± 3	13	-
SC2-P1	79 ± 5	9 ± 2	13	-
SC2-P2	76 ± 6	12 ± 4	13	-
SC2-P3	79 ± 11	<1	13	-

Data are means of triplicates ± one standard error of mean.

*For description of strains, see Table 1. Autoclaved inoculum of the wild-type strain and viable cells of mutant SC2-P4 were used as negative growth controls.

[†]Initial rate constants were measured after overnight incubation at the adjusted mixing ratio.

[‡]Final rate constants were measured at the end of the incubation periods.

[§]Growth (+), decline (-), or no change (±) in the cell numbers as determined by direct cell counts (Helber counting chamber).

wild-type strain SC2 and mutants SC2-P1, SC2-P2, and SC2-P3. These long-term incubation experiments reflected *in situ* methane concentrations more closely than growth experiments under standard laboratory conditions.

The *pmoCAB1* operon was expressed by wild-type strain SC2 and mutants SC2-P1 and SC2-P3 only at mixing ratios >600 ppmv CH₄ (Fig. 2). Correspondingly, the *pmoCAB2* mutant SC2-P3 grew and concomitantly consumed methane at concentrations ≥700 ppmv, but did not oxidize methane at concentrations ≤600 ppmv (Table 3). Therefore, the methane concentration controls the up- and down-regulation of pMMO1, and growth and concomitant oxidation of methane by wild-type strain SC2 and mutants SC2-P1 and SC2-P2 at methane concentrations <600–700 ppmv is due only to the expression of *pmoCAB2* and activity of pMMO2.

In good agreement with growth at high methane concentrations (Fig. 1A), cultures of wild-type strain SC2 and mutant SC2-P3 showed similarly high methane oxidation rate constants during incubation at 700 and 1,000 ppmv CH₄ (Table 3). The methane oxidation rate constant of mutant SC2-P1 at these CH₄ concen-

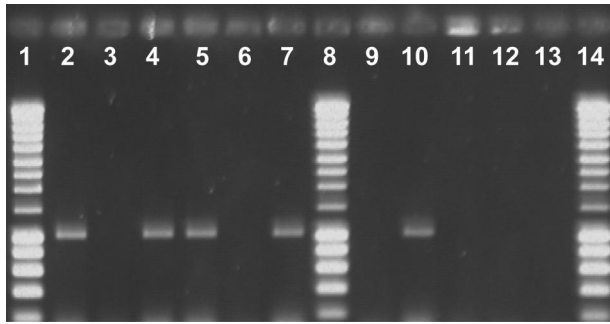


Fig. 2. Detection of *pmo* mRNA transcripts in wild-type strain SC2 and mutant strains SC2-P1, SC2-P2, and SC2-P3 after a 3-week incubation under ≥ 700 and ≤ 600 ppmv CH_4 . RT-PCR was carried out to specifically detect mRNA transcripts of either *pmoCAB1* or *pmoCAB2*. The expected size of the mRNA RT-PCR products was 1,075 bp for *pmoCAB1* and 1,056 bp for *pmoCAB2*. Lanes 1, 8, and 14, DNA size markers (Smart Ladder, Eurogentec); lanes 2–7, detection of *pmoCAB1* (lanes 2, 3, 5–7) and *pmoCAB2* (lane 4) mRNA transcripts after a 3-week incubation under ≥ 700 ppmv CH_4 ; lane 2, wild-type strain SC2; lane 3, negative control (same extract of total RNA as used for the positive control in lane 2 but without reverse transcription); lane 4, wild-type strain SC2 (same extract of total RNA from wild-type strain SC2 as in lane 2 but detection of *pmoCAB2* mRNA transcripts); lanes 5–7, mutant strains SC2-P1, SC2-P2, and SC2-P3; lanes 9–13, detection of *pmoCAB1* (lanes 9 and 11–13) and *pmoCAB2* (lane 10) mRNA transcripts after a 3-week incubation under ≤ 600 ppmv CH_4 ; lane 9, wild-type strain SC2; lane 10, wild-type strain SC2 (same extract of total RNA from wild-type strain SC2 as in lane 9 but detection of *pmoCAB2* mRNA transcripts); lanes 11–13, mutant strains SC2-P1, SC2-P2, and SC2-P3 (as exemplarily shown for wild-type strain SC2, detection of *pmoCAB2* was also positive for mutant strains SC2-P1 and SC2-P2 but not for SC2-P3 after a 3-week incubation under ≤ 600 ppmv CH_4).

trations was $\approx 50\%$ of that of wild-type strain SC2 and mutant SC2-P3 (Table 3). These findings suggest that growth and concomitant methane consumption of wild-type strain SC2 at methane concentrations ≥ 700 ppmv are mainly related to the expression of *pmoCAB1* and activity of pMMO1 and that each of the two *pmoCAB1* operons contribute 50% of the whole-cell methane oxidation activity.

Wild-type strain SC2 and the two mutants having an intact *pmoCAB2* (SC2-P1, SC2-P2) oxidized methane at mixing ratios ≤ 600 ppmv and were even able to consume atmospheric methane (1.75 ppmv) for >3 months (Table 3). Growth occurred at 100

ppmv CH_4 , and the cell numbers did not decrease during incubation under 10 ppmv CH_4 . The numbers of wild-type cells and those of mutants SC2-P1 and SC2-P2 increased ≈ 15 - to 17-fold during incubation at 100 ppmv CH_4 . These results suggested that cells of wild-type strain SC2 may be able to be maintained at methane concentrations as low as 10 ppmv and respond with growth when the methane concentration increases toward 100 ppmv.

After a 3-month incubation with atmospheric methane concentrations, wild-type strain SC2 and mutants SC2-P1 and SC2-P2 grew again when 20% methane was added to the headspace. The *pmoCAB2* mutant SC2-P3 did not resume growth under these conditions. Atmospheric concentrations of methane were oxidized when *pmoCAB2* was expressed in the wild-type strain SC2 and mutants SC2-P1 and SC2-P2, and *pmoCAB1* was not expressed in these strains under these conditions (Fig. S2). These maintenance studies thus provided unequivocal proof that consumption of atmospheric methane was caused by the activity of the pMMO2, encoded by *pmoCAB2*. *pmoCAB2* mRNA transcripts were detected in wild-type strain SC2 after incubation at all methane mixing ratios tested for the expression of *pmoCAB2*, including 1.75, 600, and 700 ppmv CH_4 , and 10–15% CH_4 (Figs. 1B and 2, Fig. S2), which indicated that *pmoCAB2* is constitutively expressed. Constitutive expression could be energetically favorable because regulation would require initiation of expression under limited growth conditions.

Methane Oxidation Kinetics. The apparent kinetics of the conventional pMMO1 could not be determined by using wild-type strain SC2 because the specific affinity (a_s^0) of pMMO1 in wild-type cells is masked by the constitutive expression of *pmoCAB2* and activity of pMMO2. $K_{m(\text{app})}$ of pMMO1 was thus derived from the methane oxidation activity of mutant SC2-P3. Pregrowth of mutant SC2-P3 at either 1,000 ppmv CH_4 or 20% CH_4 did not significantly affect $V_{\text{max}(\text{app})}$, which suggested that methane concentrations above the threshold of 600–700 ppmv induce full expression of *pmoCAB1*. The a_s^0 value was estimated from the exponential decrease of methane over time at 600–700 ppmv, resulting in a $K_{m(\text{app})}$ of 9.2–9.3 μM (Table 4).

$K_{m(\text{app})}$ of pMMO2 was derived from the methane oxidation activities of wild-type strain SC2 and mutant SC2-P2. Cells were pregrown for 4 weeks under methane concentrations <500 ppmv, thereby avoiding the expression of *pmoCAB1* in the wild-type cells. The $K_{m(\text{app})}$ values determined in both test strains were almost

Table 4. Apparent kinetic parameters [$K_{m(\text{app})}$, $V_{\text{max}(\text{app})}$, a_s^0] determined for pMMO1 (mutant SC2-P3) and pMMO2 (wild-type strain SC2, mutant SC2-P2), and threshold level of methane required for maintenance

Strain*	$K_{m(\text{app})}$, μM	$V_{\text{max}(\text{app})}$, $\times 10^{-15} \text{ mol}\cdot\text{cell}^{-1}\cdot\text{h}^{-1}$	a_s^0 , $\times 10^{-12} \text{ liter}\cdot\text{cell}^{-1}\cdot\text{h}^{-1}$	CH_4 for maintenance, ppmv [†]
Wild-type	— [§]	— [§]	—(pMMO1) [§]	1.75
	0.11 ^{¶a}	0.11 \pm 0.01 ^{¶a}	35.17 \pm 2.43 (pMMO2) ^{¶a}	
SC2-P2	0.12 ^{¶a}	0.13 \pm 0.01 ^{¶a}	34.62 \pm 1.65 (pMMO2) ^{¶a}	1.75
	2.20 ^{¶b}	2.41 \pm 0.14 ^{¶b}	37.16 \pm 1.66 (pMMO2) ^{¶b}	
SC2-P3	9.23 ^{§a}	2.00 \pm 0.11 ^{§a}	7.35 \pm 0.57 (pMMO1) ^{§a}	600–700
	9.30 ^{§b}	1.86 \pm 0.06 ^{§b}	6.78 \pm 1.30 (pMMO1) ^{§b}	

*For description of strains, see Table 1.

[†] a_s^0 describes the slope of the first-order section of a Michaelis–Menten curve and directly indicates how fast a limiting substrate is metabolized (26).

[‡]The minimum methane mixing ratios enabling cell maintenance for more than 3 months were determined experimentally.

[§] $K_{m(\text{app})}$, $V_{\text{max}(\text{app})}$, and a_s^0 of pMMO1. $K_{m(\text{app})}$ could not be determined by using wild-type strain SC2 because of the constitutive expression of *pmoCAB2*. Mutant strain SC2-P3 was pregrown at either 1,000 ppmv CH_4 (^{§a}) or 20% methane (^{§b}) to estimate $V_{\text{max}(\text{app})}$. $V_{\text{max}(\text{app})}$ was estimated from the linear decrease of methane over time by using a starting concentration of 0.4–0.5% methane in the headspace of the test tubes. The a_s^0 value of pMMO1 was derived from an exponential decrease of methane during incubation of mutant SC2-P3 at 600–700 ppmv CH_4 .

[¶] $K_{m(\text{app})}$, $V_{\text{max}(\text{app})}$, and a_s^0 of pMMO2. (^{¶a}) Wild-type strain SC2 and mutant SC2-P2 were precultured for >4 weeks at methane concentrations <500 ppmv for estimation of $V_{\text{max}(\text{app})}$. Different starting concentrations of methane in the headspace of the test tubes had no effect on $V_{\text{max}(\text{app})}$, regardless whether 500 ppmv CH_4 or 0.4–0.5% (vol/vol) methane were initially installed. (^{¶b}) $V_{\text{max}(\text{app})}$ was estimated by using cells of mutant SC2-P2 growing exponentially with 20% (vol/vol) methane. Incubation of wild-type strain SC2 and mutant SC2-P2 at 50–100 ppmv CH_4 resulted in an exponential decrease of methane, from which the a_s^0 value of pMMO2 was calculated.

Probe₁ and Probe₂, respectively (see Fig. S1 for probe design). The dot blot was first hybridized with Probe₂, stripped, and then hybridized with Probe₁ (Fig. 1B).

Growth Experiments under Low Methane Mixing Ratios. In the early exponential growth phase, wild-type strain SC2 and mutants SC2-P1, SC2-P2, and SC2-P3 were diluted to 5×10^6 cells ml⁻¹ in NH₄Cl mineral salts medium. Cell suspensions (10 ml) of wild-type strain SC2 and mutants were incubated at 25°C in 120-ml serum vials on a rotary shaker (150 rpm) under methane mixing ratios ranging from 1,000 to 10 ppmv in the headspace. The methane mixing ratios used for incubation of the three replicate cultures were lowered in 100-ppmv steps to 100 ppmv, and then to 10 ppmv. At each mixing ratio tested, fresh exponentially growing cultures were used for the 3- to 5-week incubations. In addition, maintenance was assessed at 1.75 ppmv CH₄ (3-month incubation). In these incubations, the methane mixing ratio did not fall <1.5 ppmv.

The various methane mixing ratios were adjusted and the incubations were carried out by using an experimental device described in ref. 7. In brief, the serum vials were connected to a 54-liter gas reservoir (2 × 27-liter plastigas bags, Linde) via tygon and iso-versinic tubes. The flow (0.2–2.0 liters·min⁻¹) was controlled automatically by gas flow meters coupled to membrane pumps (Fuergut); thereby keeping the installed methane concentrations in the headspace of the cultures constant. Depending on the methane-oxidizing activity of the cultures, the gas reservoir in the plastigas bags was replaced at 6- to 12-h intervals for up to 3 months. Contamination was avoided by passing the in- and out-flowing air through autoclaved cotton wool. Each culture could be disconnected from the system via two-way stopcocks to measure methane oxidation activity in closed vials.

The activity of the cultures was monitored weekly by measuring methane consumption. The methane concentrations in the headspace of the vials were determined by gas chromatography. After the incubation periods, cell viability was verified by detection of *pmo* mRNA transcripts (see below) and growth recovery under high methane concentrations. For the latter, two 10-ml replicate cultures of wild-type strain SC2 and each mutant strain were transferred into new 120-ml serum vials, mixed with 50 ml of fresh medium, and incubated under standard laboratory growth conditions with 20% CH₄ in the headspace.

RT-PCR Detection of *pmo* mRNA Transcripts. Cells were harvested by centrifugation and used immediately to detect mRNA transcripts from *pmoCAB1* and/or *pmoCAB2*. Extracts of total RNA were prepared as described in ref. 24. Reverse transcription (RT) of mRNA was carried out in a total volume of 20 μl at 56°C for 60 min by using the Omniscript RT kit (Qiagen). The reaction mixture contained 1 μl of total RNA, 0.5 mM each dNTP, reverse transcriptase buffer, 10 units of RNase inhibitor (Promega), 1.0 μM primer PmoB_{conv/nov}, and 4 units of reverse transcriptase. The primer PmoB_{conv/nov} enabled simultaneous cDNA synthesis from mRNA transcripts of both *pmoCAB1* and *pmoCAB2*. Two primer sets that specifically targeted either *pmoCAB1* or *pmoCAB2* were used to amplify the synthesized cDNA (Table S3). The reaction mixtures (100 μl total) contained: 1 μl of RT product, 10 μl of 10× reaction buffer, 1.5 mM MgCl₂, 200 μM each dNTP, 0.25 μM each primer, and 2.5 units of Taq DNA polymerase (Promega). The thermal profile was as follows: initial denaturation for 3 min at 94°C, followed by 32 cycles of denaturation at 94°C for 40 s, primer annealing at 62°C for 40 s, and elongation at 72°C for 60 s with a final extension step of 7 min. To exclude the possibility of DNA contamination, negative control reactions were carried out for all reactions in which mRNA transcripts were detected by using the same extract of total RNA without the reverse transcriptase step. Aliquots of the amplicons (10 μl) were checked by electrophoresis on a 1% agarose gel. The correct identity of the mRNA transcripts was verified by sequencing.

Methane Oxidation Kinetics [$K_{m(\text{app})}$, $V_{\text{max}(\text{app})}$, a_0^0]. The apparent kinetic parameters of conventional pMMO1 were determined with the mutant strain SC2-P3, and parameters of the pMMO2 were determined with wild-type strain SC2 and mutant SC2-P2 by using an experimental design described in ref. 7. The $V_{\text{max}(\text{app})}$ and a_0^0 values of pMMO1 and pMMO2 were determined as detailed in the footnotes to Table 4 and *SI Methods*. The $K_{m(\text{app})}$ values were calculated as $K_{m(\text{app})} = V_{\text{max}(\text{app})}/a_0^0$. Multiplication by the Oswald constant (0.03395 at 25°C) gave the $K_{m(\text{app})}$ as the methane concentration in water.

ACKNOWLEDGMENTS. We thank S. Fleissner for technical assistance; P. F. Dunfield, P. Frenzel, and C. Knief for helpful discussions; R. Conrad, S. N. Dedysh, and R. K. Thauer for critical reading of the manuscript and expert advice; and K. A. Brune for editing the manuscript. This work was supported in part by the Deutsche Forschungsgemeinschaft (SFB 395) and the Max Planck Society.

- Dlugokencky E-J, et al. (2003) Atmospheric methane levels off: Temporary pause or a new steady-state? *Geophys Res Lett* 30:1–4.
- Cicerone R-J, Oremland R-S (1988) Biogeochemical aspects of atmospheric methane. *Glob Biogeochem Cycles* 2:299–327.
- Hanson R-S, Hanson T-E (1996) Methanotrophic bacteria. *Microbiol Rev* 60:439–471.
- Heyer J, Galchenko V-F, Dunfield P-F (2002) Molecular phylogeny of type II methane-oxidizing bacteria isolated from various environments. *Microbiology* 148:2831–2846.
- Horz H-P, Tchawa Yimga M, Liesack W (2001) Detection of methanotroph diversity on roots of submerged rice plants by molecular retrieval of *pmoA*, *mmoX*, *mxhF*, and 16S rRNA and ribosomal DNA, including *pmoA*-based terminal restriction fragment length polymorphism profiling. *Appl Environ Microbiol* 67:4177–4185.
- Bender M, Conrad R (1992) Kinetics of CH₄ oxidation in oxic soils exposed to ambient air or high CH₄ mixing ratios. *FEMS Microbiol Ecol* 101:261–270.
- Knief C, Dunfield P-F (2005) Response and adaptation of different methanotrophic bacteria to low methane mixing ratios. *Environ Microbiol* 7:1307–1317.
- Harris R-C, Sebacher D-I, Day F-P, Jr (1982) Methane flux in the Great Dismal Swamp. *Nature* 297:673–674.
- Smith K-A, et al. (2000) Oxidation of atmospheric methane in Northern European soils, comparison with other ecosystems, and uncertainties in the global terrestrial sink. *Glob Change Biol* 6:791–803.
- Knief C, Lipski A, Dunfield P-F (2003) Diversity and activity of methanotrophic bacteria in different upland soils. *Appl Environ Microbiol* 69:6703–6714.
- Knief C, Kolb S, Bodelier P-L-E, Lipski A, Dunfield P-F (2006) The active methanotrophic community in hydromorphic soils changes in response to changing methane concentration. *Environ Microbiol* 8:321–333.
- Holmes A-J, et al. (1999) Characterization of methanotrophic bacterial populations in soils showing atmospheric methane uptake. *Appl Environ Microbiol* 65:3312–3318.
- Kolb S, Knief C, Dunfield P-F, Conrad R (2005) Abundance and activity of uncultured methanotrophic bacteria involved in the consumption of atmospheric methane in two forest soils. *Environ Microbiol* 7:1150–1161.
- Dedysh S-N, et al. (2000) *Methylocella palustris* gen. nov., sp. nov., a novel methane-oxidizing acidophilic bacterium from peat bogs, representing a new subtype of serine-pathway methanotrophs. *Int J Syst Evol Microbiol* 50:955–969.
- Murrell J-C, Gilbert B, McDonald I-R (2000) Molecular biology and regulation of methane monooxygenase. *Arch Microbiol* 173:325–332.
- Nielsen A-K, Gerdes K, Murrell J-C (1997) Copper-dependent reciprocal transcriptional regulation of methane monooxygenase genes in *Methylococcus capsulatus* and *Methylosinus trichosporium*. *Mol Microbiol* 25:399–409.
- Knapp C-W, Fowle D-A, Kulczycki E, Roberts J-A, Graham D-W (2007) Methane monooxygenase gene expression mediated by methanobactin in the presence of mineral copper sources. *Proc Natl Acad Sci USA* 104:12040–12045.
- Kim H-J, et al. (2004) Methanobactin, a copper-acquisition compound from methane-oxidizing bacteria. *Science* 305:1612–1615.
- Semrau J-D, et al. (1995) Particulate methane monooxygenase genes in methanotrophs. *J Bacteriol* 177:3071–3079.
- Lieberman R-L, Rosenzweig A-C (2005) Crystal structure of a membrane-bound metalloenzyme that catalyses the biological oxidation of methane. *Nature* 434:177–182.
- Balasubramanian R, Rosenzweig A-C (2007) Structural and mechanistic insights into methane oxidation by particulate methane monooxygenase. *Acc Chem Res* 40:573–580.
- Stoecker K, et al. (2006) Cohn's *Crenothrix* is a filamentous methane oxidizer with an unusual methane monooxygenase. *Proc Natl Acad Sci USA* 103:2363–2367.
- Ricke P, Erkel C, Kube M, Reinhardt R, Liesack W (2004) Comparative analysis of the conventional and novel *pmo* (particulate methane monooxygenase) operons from *Methylocystis* strain SC2. *Appl Environ Microbiol* 70:3055–3063.
- Tchawa Yimga M, Dunfield P-F, Ricke P, Heyer J, Liesack W (2003) Wide distribution of a novel *pmoA*-like gene copy among type II methanotrophs, and its expression in *Methylocystis* strain SC2. *Appl Environ Microbiol* 69:5593–5602.
- Bowman J (2006) The methanotrophs—The families *Methylococcaceae* and *Methylocystaceae*. *The Prokaryotes*, eds Dworkin M, Falkow S, Rosenberg E, Schleifer KH, Stackebrandt E (Springer, New York), Vol 5, pp 266–289.
- Button D-K (1993) Nutrient-limited microbial growth kinetics: Overview and recent advances. *Antonie van Leeuwenhoek* 63:225–235.
- Yavitt J-B, Fahey T-J, Simmons J-A (1995) Methane and carbon dioxide dynamics in a northern hardwood ecosystem. *Soil Sci Soc Am J* 59:796–804.
- Andersen B-L, Bidoglio G, Leip A, Rembges D (1998) A new method to study simultaneous methane oxidation and methane production in soils. *Global Biogeochem Cycles* 12:587–594.
- Horz H-P, et al. (2002) Activity and community structure of methane-oxidising bacteria in a wet meadow soil. *FEMS Microbiol Ecol* 41:247–257.
- Sambrook J, Russell D-W (2003) *Molecular Cloning: A Laboratory Manual* (Cold Spring Harbor Lab Press, Cold Spring Harbor, NY), 3rd Ed.
- Dunfield P-F, et al. (2002) Isolation of a *Methylocystis* strain containing a novel *pmoA*-like gene. *FEMS Microbiol Ecol* 41:17–26.